Proceedings of the World Congress on Engineering 2013 Vol I,
WCE 2013, July 3 - 5, 2013, London, U.K.

A Numerical Method for Solution of Second Order Nonlinear Parabolic Equations on a Sphere

Yuri N. Skiba, Denis M. Filatov

***Abstract*—An efficient numerical method for solution of second order nonlinear parabolic equations on a sphere is presented. The method involves the ideas of operator splitting and swap of coordinate maps for computing in different directions. As a result, 1D finite difference problems with periodic boundary conditions and matrices of a simple structure appear, so that for their solution a fast numerical algorithm is applicable. The method is tested via several numerical experiments, including simulation of the phenomena of blow-up and temperature waves, that have many important applications in industry.**

***Index Terms*—second order nonlinear parabolic equations, operator splitting, coordinate map swap, blow-up and burning processes.**

I. Introduction

SECOND order nonlinear parabolic equations are adequate mathematical models of many physical phenomena met in mechanics, biophysics, ecology and other areas of science [1], [2], [3], [4], [5], [6], [7], [8], [9]. Some of them are convenient to study in the spherical geometry separating the differential operator into the spherical and radial components. Because the radial component is trivial, in our research we shall focus on the spherical part. The model has the form

$$T_t = \nabla \cdot (\mu T^\alpha \nabla T) + f, \tag{1}$$

where ∇ is the spherical Hamilton operator, $T = T(\lambda, \varphi, t) \geq 0$, $\mu = \mu(\lambda, \varphi) > 0$, $\alpha \geq 0$, $f = f(T, \lambda, \varphi, t)$, while λ and φ are the longitude and latitude of the sphere S, respectively.

Since equation (1) is being considered on a sphere, we are dealing with a Cauchy problem formulated in a domain that has *no boundaries*. Besides, sphere is a periodic domain only in λ, while it is *not* such in φ due to the presence of the poles. Therefore, if one tries to design a numerical procedure to solve the original 2D problem using periodicity in the longitude and joining somehow the solution at the poles, it will definitely be computationally expensive. So, our aim is to develop an efficient numerical method for solving equation (1) that would allow computing physically correct numerical solutions in a fast manner.

Manuscript received March 4, 2013. This work was supported by Mexican System of Researchers (SNI) grants 14539 and 26073. It is part of the project PAPIIT DGAPA UNAM IN104811-3.

Yu.N. Skiba is with the Centro de Ciencias de la Atmosfera (CCA), Universidad Nacional Autonoma de Mexico (UNAM), Av. Universidad 3000, Cd. Universitaria, C.P. 04510, Mexico D.F., Mexico (e-mail: skiba@unam.mx).

D.M. Filatov is with Centro de Investigacion en Computacion (CIC), Instituto Politecnico Nacional (IPN), Av. Juan de Dios Batiz s/n, C.P. 07738, Mexico D.F., Mexico (phone: +52 (55) 5729-6000, ext. 56-544, fax: +52 (55) 5586-2936, e-mail: denisfi latov@gmail.com).

II. Splitting and Map Swap

Prior to performing finite difference approximation we linearise and then split the original equation by coordinates in the double time interval (t_{n-1}, t_{n+1}) [10]. So, hereafter we consider two operators, L_1—in λ, and L_2—in φ, i.e.

$$L_1 T = \frac{1}{R\cos\varphi}\frac{\partial}{\partial\lambda}\left(\frac{D}{R\cos\varphi}\frac{\partial T}{\partial\lambda}\right), \tag{2}$$

$$L_2 T = \frac{1}{R\cos\varphi}\frac{\partial}{\partial\varphi}\left(\frac{D\cos\varphi}{R}\frac{\partial T}{\partial\varphi}\right). \tag{3}$$

Here D stands for the diffusion coefficient $\mu(T^n)^\alpha$ computed at the time moment $t_n \in (t_{n-1}, t_{n+1})$, whereas R is the radius of the sphere. The corresponding split 1D problems are solved in time successively: the solution to the first problem is used as the initial condition for the second one, and vice versa.

The splitting allows one to treat the 1D problems as periodic in λ and in φ, provided each of the problems is being considered on a separate grid: the first problem is approximated on the grid

$$S^{(1)}_{\Delta\lambda,\Delta\varphi} = \left\{(\lambda_k, \varphi_l) : \lambda_k \in \left[\tfrac{\Delta\lambda}{2}, 2\pi + \tfrac{\Delta\lambda}{2}\right), \right. \\ \left. \varphi_l \in \left[-\tfrac{\pi}{2} + \tfrac{\Delta\varphi}{2}, \tfrac{\pi}{2} - \tfrac{\Delta\varphi}{2}\right]\right\}, \tag{4}$$

while the second one is approximated on the swapped grid

$$S^{(2)}_{\Delta\lambda,\Delta\varphi} = \left\{(\lambda_k, \varphi_l) : \lambda_k \in \left[\tfrac{\Delta\lambda}{2}, \pi - \tfrac{\Delta\lambda}{2}\right], \right. \\ \left. \varphi_l \in \left[-\tfrac{\pi}{2} + \tfrac{\Delta\varphi}{2}, \tfrac{3\pi}{2} + \tfrac{\Delta\varphi}{2}\right)\right\}. \tag{5}$$

Obviously, both grids are defined on the same set of nodes. The only change to make in (3) if using (5) is to replace $\cos\varphi$ with $|\cos\varphi|$, as well.

Now we are ready to construct finite difference approximations of the derived 1D problems. To obtain the second approximation order in time, the bicyclic splitting [10] (a sort of Strang splittings [11]) is used in each double time interval (t_{n-1}, t_{n+1}) coupled with the Crank-Nicolson approximation—

$$T^{n-1+i/3}_{kl} - T^{n-(4-i)/3}_{kl} = \\ \tau L_i\left(\frac{T^{n-1+i/3}_{kl} + T^{n-(4-i)/3}_{kl}}{2}\right), \quad i = 1, 2, \tag{6}$$

$$T^{n+1/3}_{kl} - T^{n-1/3}_{kl} = 2\tau f^n_{kl}, \tag{7}$$

$$T^{n+(4-i)/3}_{kl} - T^{n+(3-i)/3}_{kl} = \\ \tau L_i\left(\frac{T^{n+(4-i)/3}_{kl} + T^{n+(3-i)/3}_{kl}}{2}\right), \quad i = 2, 1, \tag{8}$$

ISBN: 978-988-19251-0-7
ISSN: 2078-0958 (Print); ISSN: 2078-0966 (Online)

where the external forcing f is computed as $f_{kl}^n = f(\lambda_k, \varphi_l, t_n)$. Further, at each point (λ_k, φ_l) the spatial derivatives of the operators L_i are approximated as

$$\frac{\partial}{\partial\lambda}\left(D\frac{\partial T}{\partial\lambda}\right) \approx \frac{1}{(\Delta\lambda)^2}\left(D^+\nabla_k^+ T_{kl} - D^-\nabla_k^- T_{kl}\right), \quad (9)$$

$$\frac{\partial}{\partial\varphi}\left(\overline{D}\frac{\partial T}{\partial\varphi}\right) \approx \frac{1}{(\Delta\varphi)^2}\left(\overline{D}^+\nabla_l^+ T_{kl} - \overline{D}^-\nabla_l^- T_{kl}\right), \quad (10)$$

where $D^+ = (D_{k+1,l} + D_{kl})/2$, $D^- = (D_{kl} + D_{k-1,l})/2$, $\nabla_k^+ T_{kl} = T_{k+1,l} - T_{kl}$, $\nabla_k^- T_{kl} = T_{kl} - T_{k-1,l}$, $\overline{D} = D\,|\cos\varphi|$, $\overline{D}^+ = (\overline{D}_{k,l+1} + \overline{D}_{kl})/2$, $\overline{D}^- = (\overline{D}_{kl} + \overline{D}_{k,l-1})/2$, $\nabla_l^+ T_{kl} = T_{k,l+1} - T_{kl}$, $\nabla_l^- T_{kl} = T_{kl} - T_{k,l-1}$.

It can explicitly be shown that each of the resulting split one-dimensional second order finite difference schemes is dissipative. More generally, it holds

$$||\mathbf{T}^{n+1}||_{L_2\left(S^{(1)}_{\Delta\lambda,\varphi_l}\right)} \le ||\mathbf{T}^{n-1}||_{L_2\left(S^{(1)}_{\Delta\lambda,\varphi_l}\right)} + 2\tau||\mathbf{f}^n||_{L_2\left(S^{(1)}_{\Delta\lambda,\varphi_l}\right)}, \quad (11)$$

where $\mathbf{T} = \{T_{kl}\}$ and $\mathbf{f} = \{f_{kl}\}$ are grid functions taken at the corresponding time moments. Besides, it is easy to demonstrate that the schemes result to be balanced.

Let us emphasise that a substantial profit we have achieved due to the splitting is that we use periodic boundary conditions while computing in *both* directions, λ and φ, thus having finite difference schemes with tridiagonal matrices. Therefore, the solution can be obtained with a fast linear solver, so it is cheap from the computational standpoint.

Another gain of the splitting is that one can take higher than second order finite difference stencils and hence derive higher order finite difference schemes.

III. Numerical Tests

A. Test for the Balance Property

Let the function

$$T(\lambda, \varphi, t) = c_1 \sin\xi \cos\varphi \cos^2 t + c_2 \quad (12)$$

with

$$\xi = \omega\lambda + \theta\cos\kappa\varphi \sin t \quad (13)$$

be the solution to (1). Then, having found the corresponding source function f via a substitution of (12) into (1), we can solve the diffusion problem numerically and compare the solution with the known analytics.

In doing so, we take $c_1 = -2.5$, $c_2 = 50$, $\omega = 9$, $\theta = 5$, $\kappa = 3$, $\alpha = 1$, $\mu = 10^{-5}$. In Fig. 1 we plot graphs of the temporal behaviour of the total mass of the solution, computed on the grid $6^\circ \times 6^\circ$, and the source function. As one can see, the total mass is decaying when the (negative) sources are growing; when the sources are about zero, the total mass is nearly a constant, as it ought to be. This result demonstrates that the constructed schemes possess the property of balance and hence provide physically adequate numerical solutions. Maximum relative error of the numerical solution is $\delta(t_n) = 0.54\%$ at $\tau = 10^{-3}$, as well.

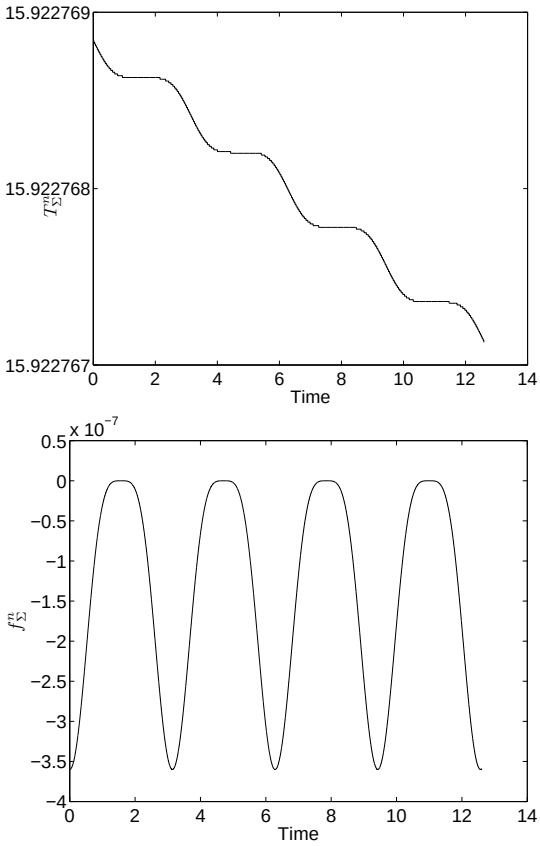

Fig. 1. Balance Property Test: graphs of the total mass (top) and sources (bottom) in time

B. Test of Combustion and Temperature Waves

Now we are going to verify the schemes on modelling two strongly nonlinear real physical phenomena. The first phenomenon is the propagation of a temperature wave at a constant amplitude; the second phenomenon is combustion in a limited area, one of whose applications is metal surface flaming. Both phenomena were numerically simulated in [1], [2] as Cauchy problems on $\mathbb{R}^1$. Below we shall apply the constructed schemes for studying them on a sphere.

Temperature wave. Take $\alpha = 0$, $\mu = 10^{-4}$ and $f = c(T - T^3)$ with $c = 10$. This problem is linear with respect to the diffusion coefficient, but it is nonlinear with respect to the source function. We shall consider two cases, taking a hat-like spot as the initial condition: in the first case the spot's epicentre is located in middle latitudes, while in the second case it is placed exactly on the North pole. The numerical solutions, obtained on the grid $6^\circ \times 6^\circ$, are shown in Fig. 2-3. There are two features to notice. First, as the time is growing the wave fronts are covering the entire sphere, while the waves' amplitudes are kept constant in time (cf. the colourbar's values at different time moments), that is temperature waves at constant amplitudes are observed. Second, the phenomenon is accurately simulated independently of the location of the initial condition, without any perturbances of the solution which would have taken place if we had added any nonphysical modes into the model at the stage of splitting and/or map swap (4)-(5).

Combustion within a limited area. Let $\alpha = 1$ and $f = cT^\beta$, where $c = 4.5$. The model is now nonlinear both with respect to the diffusion coefficient and sources. The

ISBN: 978-988-19251-0-7
ISSN: 2078-0958 (Print); ISSN: 2078-0966 (Online)

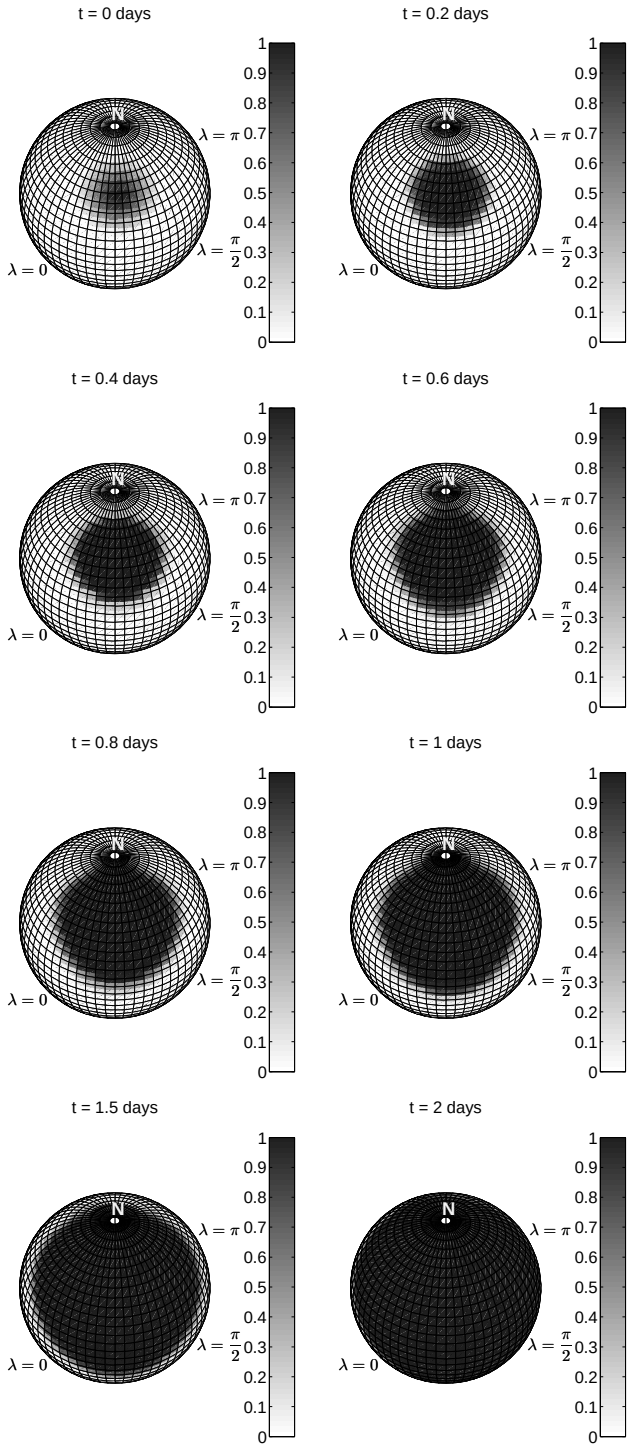

Fig. 2. Temperature Wave Test: mid-lat numerical solution at several time moments

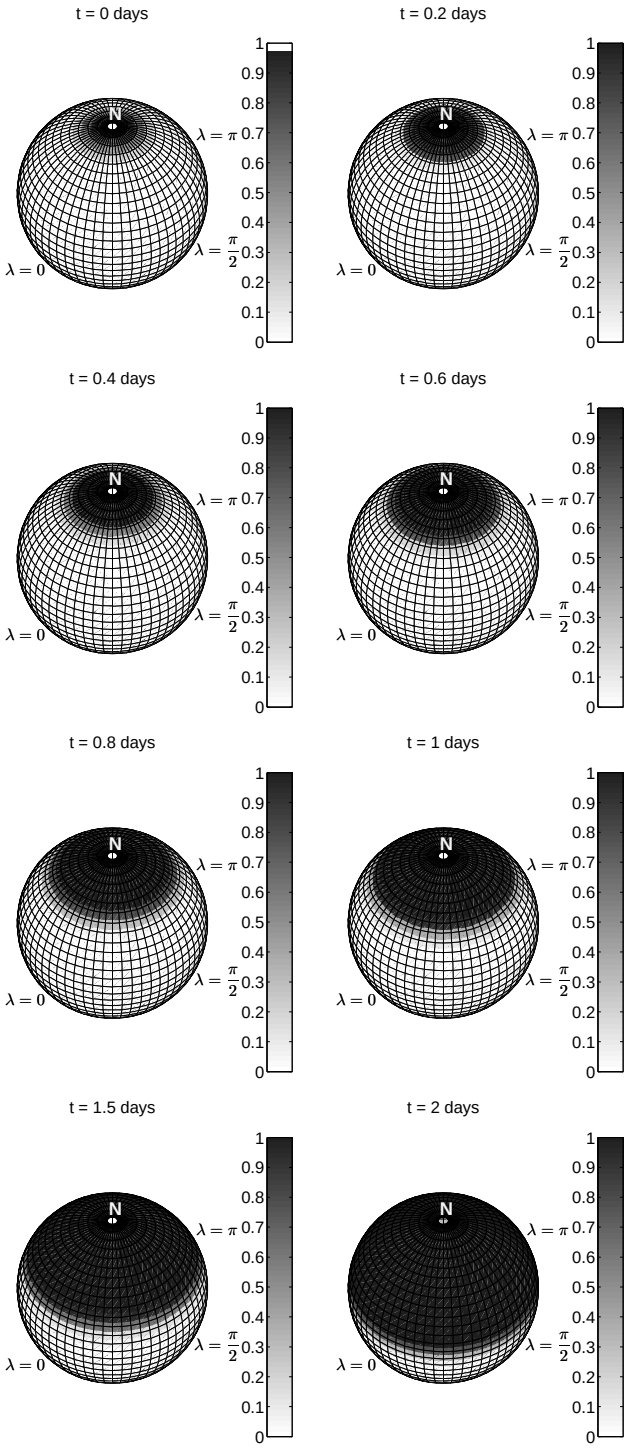

Fig. 3. Temperature Wave Test: North pole numerical solution at several time moments

parameter β determines distinct regimes of combustion: the case $0 < \beta < \alpha + 1$ is the expansion regime (or HS-regime [1], [2])—the area of combustion is getting larger in time; the case $\beta > \alpha + 1$ is the reduction regime (or LS-regime)—the area of combustion is getting smaller; the case $\beta = \alpha + 1$ is the stationary regime (S-regime), when combustion is limited within an area of a constant size. In all three cases the source function leads to an infinite increase of the temperature T, that is a blow-up occurs.

In Fig. 4 we show the initial condition, while in Fig. 5-7 there are numerical solutions corresponding to $\beta = 1$ (HS-regime), $\beta = 3$ (LS-regime) and $\beta = 2$ (S-regime), respectively. In Fig. 8 we plot graphs of the solutions' L_2-norms. It is seen that a blow-up is tended to be achieved in all the cases—the solutions' amplitudes unboundedly grow in time, while the behaviour of the combustion area depends on the parameter β and agrees with the theory. Hence, the constructed schemes allow properly simulating all the regimes of combusion, including the border sensitive S-regime.

ISBN: 978-988-19251-0-7
ISSN: 2078-0958 (Print); ISSN: 2078-0966 (Online)

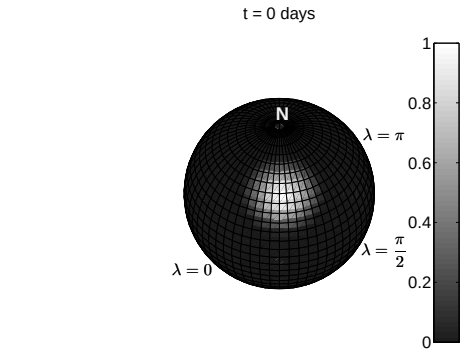

Fig. 4. Combustion Test: initial condition

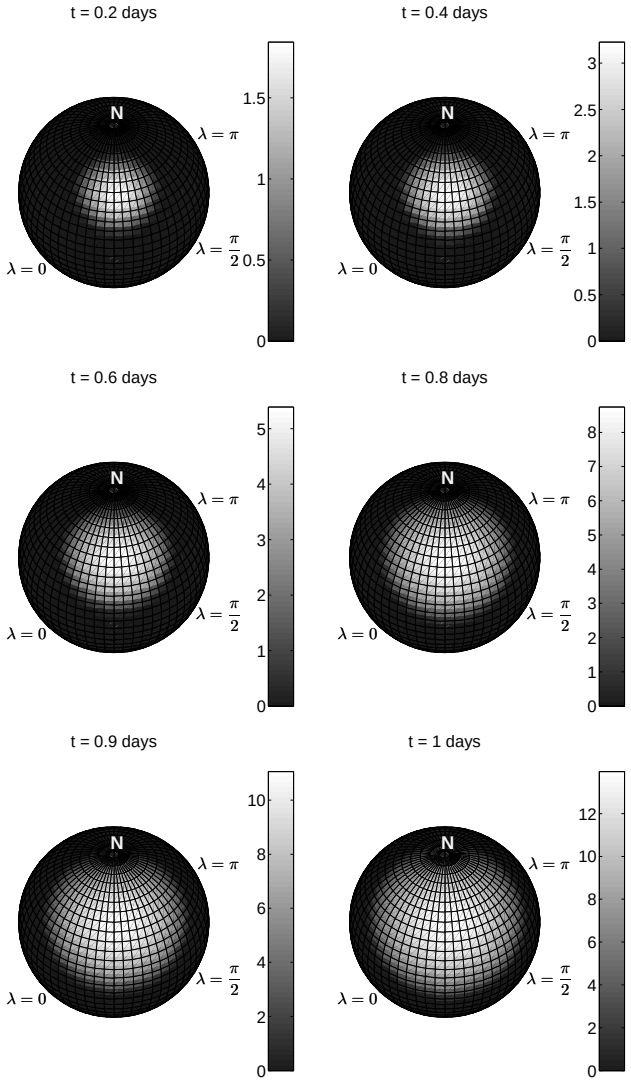

Fig. 5. Combustion Test: numerical solution for HS-regime at several time moments

IV. Conclusion

A numerical method for solution of nonlinear parabolic equations on a sphere has been presented. The keypoint of the method is the operator splitting by coordinates and subsequent map swap that allows representing the sphere as if it were a periodic domain in both directions. Hence, we constructed second order finite difference schemes approximating 1D diffusion problems with periodic boundary conditions in the longitude and latitude. Therefore we avoided difficulties related to imposing suitable boundary conditions at the poles. The constructed schemes keep the significant properties of the original differential problem—they are balanced and dissipative, and thus provide physically adequate numerical solutions. Due to the tridiagonal structure of the matrices of the linear systems the schemes are computationally inexpensive. The numerical experiments demonstrated accurate simulation of two important physical phenomena—temperature waves and combustion with blow-up.

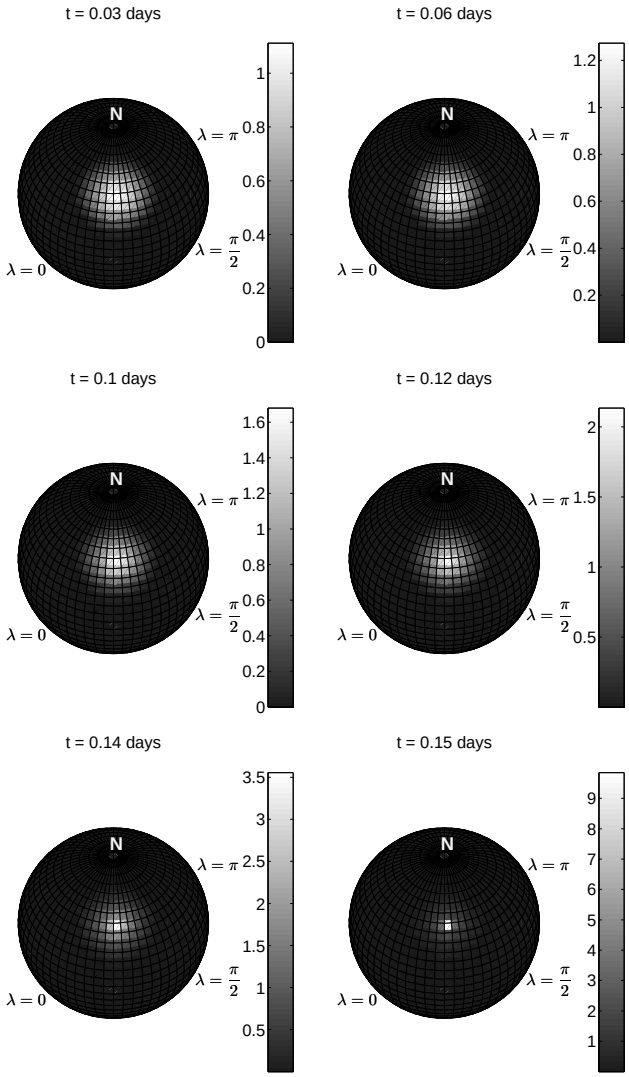

Fig. 6. Combustion Test: numerical solution for LS-regime at several time moments

References

[1] A. A. Samarskii *et al.*, *Blow-up in Quasilinear Parabolic Equations*, Walter de Gruyter, 1995.

[2] A. A. Samarskii *et al.*, "Thermal Structures and the Fundamental Length in a Medium with Nonlinear Heat Conductivity and Volume Heat Sources", in: *Regimes with Sharpening. An Evolution of the Idea. Co-evolution Laws of Complex Structures*, Nauka: Moscow, 1999, pp. 39-46 (in Russian).

[3] J. Bear, *Dynamics of Fluids in Porous Media*, Courier Dover Publications, 1988.

[4] M. E. Glicksman, *Diffusion in Solids: Field Theory, Solid-State Principles and Applications*, John Wiley & Sons, 2000.

ISBN: 978-988-19251-0-7
ISSN: 2078-0958 (Print); ISSN: 2078-0966 (Online)

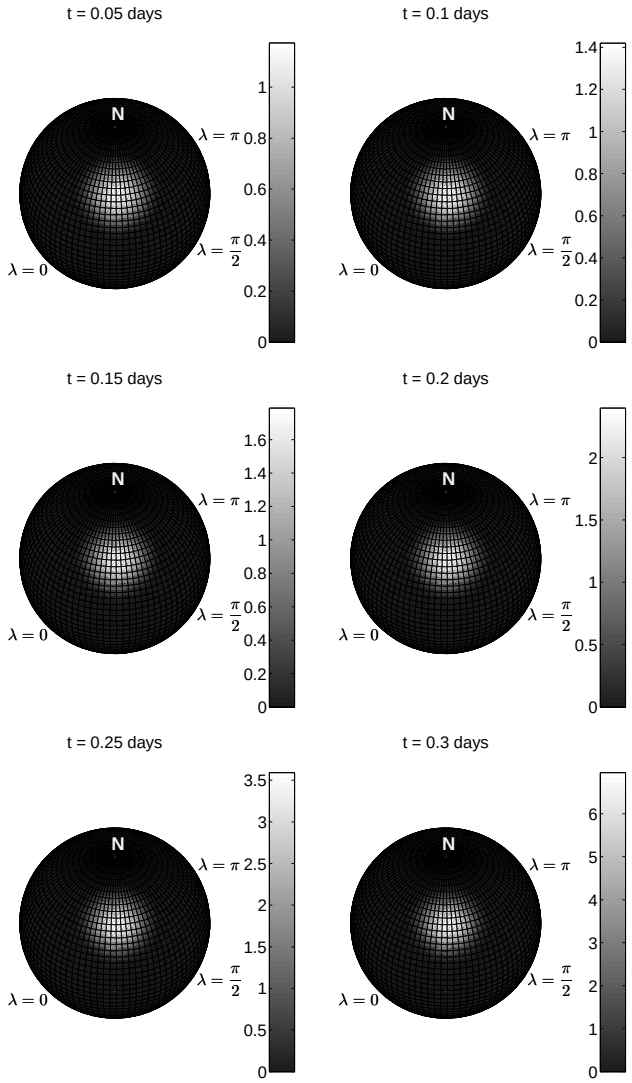

Fig. 7. Combustion Test: numerical solution for S-regime at several time moments

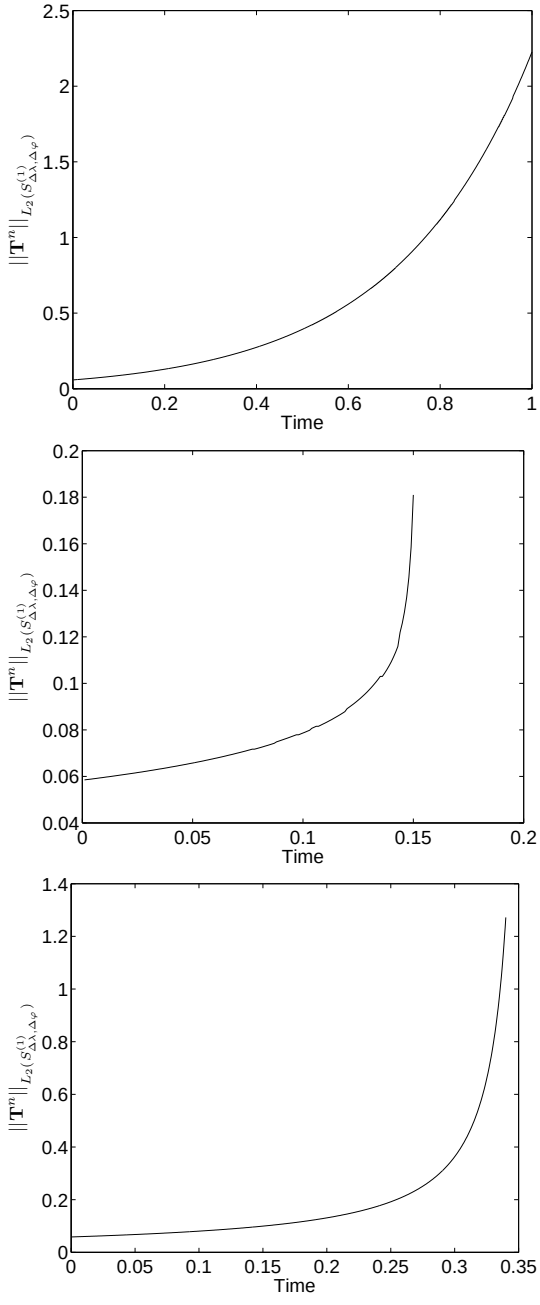

Fig. 8. Combustion Test: graphs of the L_2-norms of the solutions in time for HS- (top), LS- (middle) and S- (bottom) regimes

[5] J. R. King, "'Instantaneous Source' Solutions to a Singular Nonlinear Diffusion Equation," *Journal of Engineering Mathematics*, vol. 27, 1993, pp. 31-72.
[6] A. A. Lacey, J. R. Ockerdon, A. B. Tayler, "'Waiting-time' Solutions of a Nonlinear Diffusion Equation," *SIAM Journal of Applied Mathematics*, vol. 42, 1982, pp. 1252-1264.
[7] G. A. Rudykh, E. I. Semenov, "Non-self-similar Solutions of Multidimensional Nonlinear Diffusion Equations," *Mathematical Notes*, vol. 67, 2000, pp. 200-206.
[8] A. Kh. Vorob'yov, *Diffusion Problems in Chemical Kinetics*, Moscow University Press, 2003 (in Russian).
[9] Z. Wu *et al.*, *Nonlinear Diffusion Equations*, World Scientifi c Publishing: Singapore, 2001.
[10] G. I. Marchuk, *Methods of Computational Mathematics*, Springer, 1982 (translated from Russian, Nauka: Moscow, 1977).
[11] G. Strang, "On the Construction and Comparison of Difference Schemes," *SIAM Journal of Numerical Analysis*, vol. 5, 1968, pp. 506-517.

ISBN: 978-988-19251-0-7
ISSN: 2078-0958 (Print); ISSN: 2078-0966 (Online)